

# Comprehensive Study of the Electron Scattering Mechanisms in 4H-SiC MOSFETs

V. Uhnevionak, A. Burenkov, C. Strenger, G. Ortiz, *Member, IEEE*, E. Bedel-Pereira, V. Mortet, F. Cristiano, A. J. Bauer, and P. Pichler, *Senior Member, IEEE*

**Abstract**—The effects of doping concentration and temperature upon the transport properties in the channel of lateral n-channel SiC MOSFETs have been studied using current-voltage and Hall-effect measurements. To interpret the electrical measurements, numerical TCAD simulations have been performed. A simulation methodology which includes the calculation of the Hall factor in the channel of SiC MOSFETs has been developed and applied. In addition, a new model for the bulk mobility has been suggested to explain the temperature dependence of the MOSFET characteristics with different background doping concentrations. Based on the good agreement between the simulated and measured results, scattering mechanisms in the channel of SiC MOSFETs have been studied.

**Index Terms**—SiC MOSFET, electron mobility, scattering mechanisms, Hall effect.

## I. INTRODUCTION

4H-SiC is a wide bandgap semiconductor that possesses a favorable combination of physical properties making it attractive for various applications in the electronic industry. Its wide bandgap, high thermal conductivity, high saturation velocity and high electric breakdown field makes it the material of choice for power electronics. In addition, the ability to form SiO<sub>2</sub> on SiC by thermal oxidation in a way similar to Si provides a good basis for the fabrication of SiC MOS-based electronic devices. However, despite the similarity of the oxides grown on Si and SiC, the oxidation process of SiC is different due to the presence of carbon and leads to a higher density of interface traps. For comparison, the density of interface traps at the Si/SiO<sub>2</sub> interface in modern CMOS technology does not exceed 10<sup>10</sup> cm<sup>-2</sup>/eV. In contrast, at the SiC/SiO<sub>2</sub> interface, this value is about ~10<sup>11</sup> cm<sup>-2</sup>/eV in the middle of the bandgap and

Manuscript received XX.XX.2015. This work has been carried out in the framework of the project MobiSiC (Mobility engineering for SiC devices) and supported partly within the Program Inter Carnot Fraunhofer (PICF 2010) by the BMBF (Grant 01SF0804) and the ANR, as well as by the French RENATECH network and the J.E. Purkyně fellowship awarded to V. Mortet by the Academy of Sciences of the Czech Republic.

V. Uhnevionak, A. Burenkov, C. Strenger, A. J. Bauer and P. Pichler are with the Fraunhofer IISB, 91058 Erlangen, German (email: [alex.burenkov@iisb.fraunhofer.de](mailto:alex.burenkov@iisb.fraunhofer.de), [anton.bauer@iisb.fraunhofer.de](mailto:anton.bauer@iisb.fraunhofer.de), [peter.pichler@iisb.fraunhofer.de](mailto:peter.pichler@iisb.fraunhofer.de)).

G. Ortiz, E. Bedel-Pereira, and F. Cristiano are with LAAS-CNRS, BP 54200, 31031 Toulouse, France (email: [guillermo.ortiz@cea.fr](mailto:guillermo.ortiz@cea.fr), [elena@laas.fr](mailto:elena@laas.fr), [cfuccio@laas.fr](mailto:cfuccio@laas.fr)).

V. Mortet is with the Academy of Sciences of the Czech Republic, Prague, Czech Republic (email: [mortetv@fzu.cz](mailto:mortetv@fzu.cz)).

10<sup>13</sup> cm<sup>-2</sup>/eV or even more at the band edges of 4H-SiC [1], [2]. The quality of the interface between the semiconductor and the gate oxide is a critical factor for the device performance of MOSFETs with a surface channel. For example, the performance of lateral 4H-SiC MOSFETs is very low because of the low channel mobility. This is usually explained by the high density of interface traps which lead to strong Coulomb scattering at the interface charges and, thus, reduce significantly the channel mobility. For its improvement the impact of Coulomb scattering at the charged interface traps has to be reduced. Currently, the main strategy for a reduction of the aforementioned scattering mechanism is based on methodologies for the passivation of the interface traps, e.g. by nitridation [3], [4]. However, in addition, the amount of charged interface traps which affect the performance of MOSFETs can be controlled by changing the background doping concentration  $N_A$  [5]–[7].

In this work, the effects of doping concentration and temperature upon the transport properties in the channel of SiC MOSFETs have been studied. For this purpose, lateral 4H-SiC n-channel MOSFETs have been manufactured and electrically characterized by current-voltage as well as by Hall-effect measurements. The main finding of this work is that a change of the background doping concentration changes also the temperature dependence of the transport properties of SiC MOSFETs. To interpret the results of the measurements, numerical simulations have been performed with Sentaurus Device of Synopsys. For this, a simulation methodology has been developed and applied. Based on the good agreement between simulations and measurements, a comprehensive study of the scattering mechanisms in the channel with different doping concentrations and at different temperatures has been carried out. For a quantitative comparison between the contributions of the scattering mechanisms in the channel mobility of SiC MOSFETs, the dependence of the Hall mobility on the effective electric field has been calculated and is discussed.

## II. TEST STRUCTURES

Lateral n-channel 4H-SiC MOSFETs have been fabricated on p-type 4<sup>o</sup>-off 4H-SiC (0001) Si-face substrates with aluminum concentrations  $N_A$  of 1·10<sup>15</sup> cm<sup>-3</sup>, 1·10<sup>16</sup> cm<sup>-3</sup>, 5·10<sup>16</sup> cm<sup>-3</sup>, and 5·10<sup>17</sup> cm<sup>-3</sup>. The channel length and width of the MOSFETs were 500 μm and 80 μm, respectively. To obtain Al concentrations of 1·10<sup>16</sup> cm<sup>-3</sup> and 5·10<sup>16</sup> cm<sup>-3</sup>, box-shaped, p-type wells were fabricated by multiple Al-implantations into the epitaxial layer which had a background acceptor

concentration of  $1 \cdot 10^{15} \text{ cm}^{-3}$ . The gate oxide was grown by thermal oxidation in  $\text{N}_2\text{O}$  atmosphere at 1550 K and annealed at the same temperature for 30 min in an  $\text{N}_2$  ambient. The oxidation time for the MOSFET with the background doping concentration of  $5 \cdot 10^{17} \text{ cm}^{-3}$  was 180 min and lead to a thickness of the gate oxide of 34 nm. For the other MOSFETs, the oxidation time was 150 min which resulted in a gate oxide thickness of 25.5 nm.

To characterize the MOSFETs electrically, current-voltage and Hall-effect measurements were performed. The MOSFETs with the Al-doping concentrations of  $1 \cdot 10^{16} \text{ cm}^{-3}$  and  $5 \cdot 10^{16} \text{ cm}^{-3}$  have been characterized at room temperature (300 K). The MOSFETs with  $N_A$  values of  $1 \cdot 10^{15} \text{ cm}^{-3}$  and  $5 \cdot 10^{17} \text{ cm}^{-3}$  have been additionally characterized in the temperature range from 150 to 500 K. The source-drain voltage  $V_D$  in the current-voltage and in the Hall-effect measurements was set to 0.1 V and the gate voltage was varied between 0 and 20 V. The Hall-effect measurements were carried out using a permanent magnet with a magnetic field of 0.33 T. The choice of the low  $V_D$  allows to focus on the linear mode of operation of the SiC MOSFETs avoiding the problems of high-field electron transport. From the results of the Hall-effect measurements the Hall mobility  $\mu_H$  and the drift-channel mobility  $\mu$  as well as the sheet carrier density of electrons  $n_{inv}$  in the inversion layer were determined as a function of gate voltage  $V_G$  from the measurable quantities considering the Hall factor  $r_H$  by the formulas

$$\mu_H = \frac{V_H}{\rho I_D B} \quad (1)$$

$$\mu = \frac{\mu_H}{r_H} \quad (2)$$

$$n_{inv} = r_H \frac{I_D B}{q V_H} \quad (3)$$

Therein,  $I_D$  denotes the drain current,  $B$  the magnetic field,  $q$  the elementary charge,  $V_H$  the Hall-effect voltage, and  $\rho$  the channel resistivity.

To complement the Hall measurements for the evaluation of the interface trap density, capacitance-voltage measurements have been performed on a substrate oxidized in a similar way as the MOSFETs.

More details of the fabrication process as well as the measurement setup can be found elsewhere [7], [8].

### III. EXPERIMENTAL RESULTS

It is widely accepted that the channel mobility in lateral MOSFETs, in particular in SiC MOSFETs, is determined by the following scattering mechanisms: Coulomb scattering at ionized impurities in the bulk and at interface charges, surface-roughness scattering, as well as surface-phonon and bulk-phonon scattering [9], [10]. In Si MOSFETs, it was found that the electron channel mobility shows a universal behavior at high electric fields when plotted as a function of the effective electric field normal to the semiconductor surface. Processing and device conditions as well as doping concentrations do not affect the channel mobility in this

regime significantly [11]. This result was taken as evidence that the channel mobility of Si MOSFETs is predominantly limited by surface-phonon scattering.

For a first, qualitative assessment whether something similar can be found in SiC, the field dependence of the Hall mobility has been drawn in Fig. 1 for the available MOSFETs as a function of the effective normal electric field  $E_{eff}$ . Following [11],  $E_{eff}$  has been calculated from

$$E_{eff} = \frac{q}{\epsilon_S} \left( N_A x_d + \frac{1}{\eta} n_{inv} \right). \quad (4)$$

with  $\epsilon_S$  being the dielectric constant of the semiconductor and  $x_d$  the depletion width given by

$$x_d = \sqrt{\frac{4 \epsilon_S k T \ln(N_A/n_i)}{q^2 N_A}} \quad (5)$$

where  $k$  is Boltzmann's constant,  $T$  the absolute temperature, and  $n_i$  the intrinsic charge carrier concentration. For Fig. 1, a value of 2 was assumed for  $\eta$ . In addition to the mobility curves, asymptotic trends of the mobility components associated with surface-roughness scattering  $\mu_{SR} \sim E^{-2}$  and with surface-phonon scattering  $\mu_{SP} \sim E^{-1/3}$  have been included for comparison.

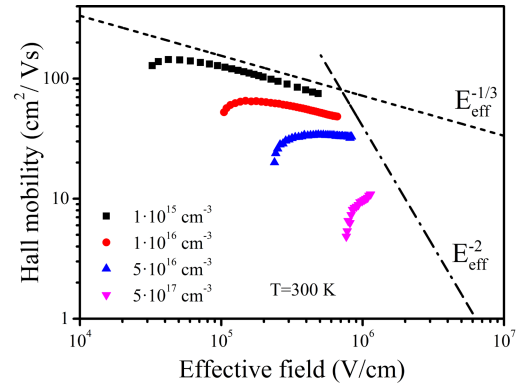


Fig. 1. Dependence of the measured Hall mobility on the effective normal electrical field for the studied MOSFETs with their different background doping concentrations.

In Fig. 1 it can be seen that the measured Hall mobility values of the inversion electrons in the channel do not lie on a common curve at high electric fields. At least for the studied range of electric fields, this allows us to conclude that it is not just surface-phonon scattering as in silicon that limits the high-field mobility in SiC. However, it is interesting to note that the Hall mobility of the lightest doped MOSFET reproduces the  $E^{-1/3}$  dependence for a wide range of electric fields. The same trend is observed to an increasingly smaller degree for higher doping concentrations. Going to lower effective field values, the Hall mobility decreases after a maximum. This indicates a change in the dominant scattering mechanism. The field dependence of the MOSFET with the highest doping concentration of  $5 \cdot 10^{17} \text{ cm}^{-3}$  apparently reflects only the low-field branch. An increase of  $\mu_H$  with the effective field as observed for low electric fields would be expected for dominant Coulomb scattering at interface charges.

To better identify the dominant scattering mechanism, the field dependences of the Hall mobility have been evaluated for the MOSFETs with the lowest and highest  $N_A$ , i.e.  $1 \cdot 10^{15} \text{ cm}^{-3}$  and  $5 \cdot 10^{17} \text{ cm}^{-3}$ , at different temperatures. Here it should be noted that each kind of scattering mechanisms has its specific temperature dependence. As an example, with an increase in temperature, Coulomb scattering decreases but phonon scattering increases. The effects on the respective mobility are vice versa. The dependence of the Hall mobility on the effective field is shown in Fig. 2 for the MOSFET with  $N_A = 1 \cdot 10^{15} \text{ cm}^{-3}$  in the temperature range from 150 K till 500 K.

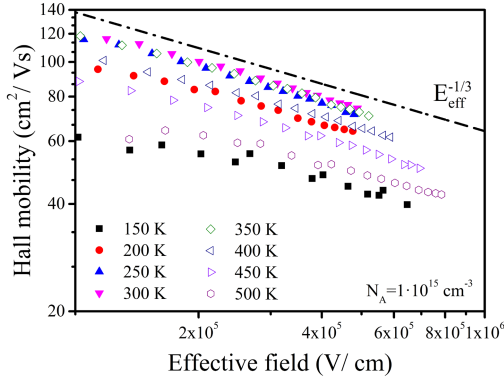


Fig. 2. Temperature and field dependence of the measured Hall mobility for the MOSFET with the lowest background doping concentration.

While all curves in Fig. 2 follow approximately the  $E^{-1/3}$  trend line associated with surface-phonon scattering, it is interesting to note that the Hall mobility increases for all fields from 150 K till 300 K while it decreases again for higher temperatures. Similar results have been obtained in the work of Lu and et al. [12]. They showed that a suitable variation of process conditions led to a strong decrease of Coulomb scattering at interface charges and consequently to a dominance of phonon scattering and an associated decrease of the field-effect mobility with temperature.

For the MOSFET with  $N_A = 5 \cdot 10^{17} \text{ cm}^{-3}$  the dependence of the Hall mobility on the effective field is shown in Fig. 3 in the temperature range from 175 K till 400 K.

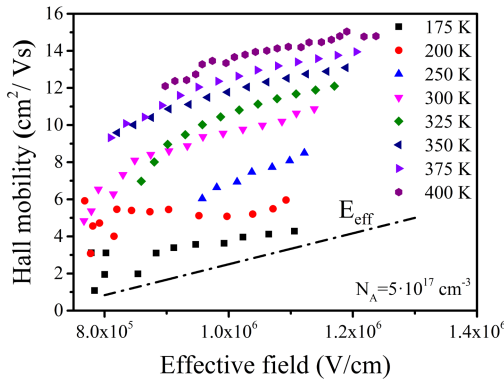


Fig. 3. Temperature dependence of the measured Hall mobility with the effective electric field for the MOSFET with the highest background doping concentration.

In contrast to the Hall mobility of the MOSFET with the lowest  $N_A$ , the Hall mobility for the MOSFET with the highest

$N_A$  shows a continuous increase with increasing temperature from 175 K till 400 K following the asymptotic trend line  $\sim E_{eff}$ . Particularly the temperature dependence of  $\mu_H$  confirms the statement that Coulomb scattering at the interface charges dominates for the highly doped MOSFETs. This is also in agreement with results of Tilak and et al. [13].

#### IV. SIMULATION RESULTS

The temperature dependence of the Hall mobility at the different doping concentrations can be better understood by analyzing the scattering mechanisms contributing to the channel mobility. In this work, the available experimental data have been reproduced first using numerical simulations with Sentaurus Device. Then, the electron mobility components associated with the main scattering mechanisms have been extracted from the numerical device simulation and analyzed. Because of convergence problems at low temperatures and the higher priority of elevated temperatures, the measurements below room temperature have not been further used in view of the limited project resources.

##### A. Simulation model

Taking into account that low channel mobilities in lateral SiC MOSFETs are usually explained by Coulomb scattering at interface charges, accurate models for the interface traps and the mobility degradation are of vital importance for the simulation. To obtain the energetic distribution of interface traps, an improved procedure was used [14]. At first, an approximate distribution of traps versus trap energy was extracted from Hall-effect [15] and complementary capacitance-voltage measurements. This was then used directly in Sentaurus Device via a table function and optimized to reproduce the three experimentally measured characteristics by simulation:  $I_D(V_G)$ ,  $n_{inv}(V_G)$  and  $\mu(V_G)$ . The mobility degradation model used in the simulations accounts for scattering mechanisms associated with Coulomb scattering at the ionized impurities in the bulk  $\mu_{IMP}$  and at the interface charges  $\mu_C$ , surface-roughness  $\mu_{SR}$ , surface-phonon  $\mu_{SP}$  and bulk-phonon scattering  $\mu_{BP}$ . The total channel mobility is assumed to result from Matthiessen's rule as

$$\frac{1}{\mu} = \frac{1}{\mu_{IMP}} + \frac{1}{\mu_{BP}} + \frac{1}{\mu_C} + \frac{1}{\mu_{SR}} + \frac{1}{\mu_{SP}} \quad (6)$$

Therein, the contributions from Coulomb scattering at ionized impurities  $\mu_{IMP}$  and bulk-phonon scattering  $\mu_{BP}$  are usually combined to the bulk mobility  $\mu_B$

$$\frac{1}{\mu_B} = \frac{1}{\mu_{IMP}} + \frac{1}{\mu_{BP}} \quad (7)$$

In this work, to simulate the temperature dependence of the electrical characteristics of the studied MOSFETs with low and high background doping concentrations, a new model for the bulk mobility component  $\mu_B$  was developed on the basis of the conventional one [16], [17] and implemented into Sentaurus Device in the form

$$\mu_B = \mu_{min} \left( \frac{T}{300 \text{ K}} \right)^\alpha + \frac{\mu_{BP} - \mu_{min} \left( \frac{T}{300 \text{ K}} \right)^\alpha}{1 + \left( \frac{T}{300 \text{ K}} \right)^\vartheta \left( \frac{N_A}{N_{ref}} \right)^z} \quad (8)$$

with the temperature dependence of the bulk-phonon related mobility  $\mu_{BP}$  defined as a sum of two terms

$$\mu_{BP} = \mu_{BP1} \left( \frac{T}{300 \text{ K}} \right)^\xi + \mu_{BP2} \left( \frac{T}{300 \text{ K}} \right)^\varkappa \quad (9)$$

Therein,  $\mu_{min}$  is the minimum value of the bulk mobility at high doping concentration at 300 K,  $N_{ref}$ ,  $\alpha$ ,  $\vartheta$ ,  $z$ ,  $\xi$ , and  $\varkappa$  are fitting parameters. The values of the model parameters used in the simulations can be found in Table I.

TABLE I  
PARAMETER VALUES FOR THE TEMPERATURE-DEPENDENT BULK MOBILITY MODEL FOR 4H-SiC [14], [16], [17]

Symbol	Value	Units
$\mu_{min}$	40	cm <sup>2</sup> /Vs
$\mu_{BP1}$	500	cm <sup>2</sup> /Vs
$\mu_{BP2}$	450	cm <sup>2</sup> /Vs
$N_{ref}$	$2 \cdot 10^{17}$	cm <sup>-3</sup>
$\alpha$	-0.5	1
$\xi$	-11.6	1
$\varkappa$	-2.74	1
$\vartheta$	-12.5	1
$z$	0.76	1

Development of the new model (8) has been based on an analysis of scattering mechanisms in the channel of the SiC MOSFETs with  $N_A$  values of  $1 \cdot 10^{15}$  cm<sup>-3</sup> and of  $5 \cdot 10^{17}$  cm<sup>-3</sup> with Sentaurus Device at different temperatures. It was found that bulk-phonon scattering in SiC has to increase stronger with temperature than it was predicted by the conventional model developed originally for Si. This has been implemented by the description of the mobility component  $\mu_{BP}$  via two terms, as it is shown in (9), instead of the conventional description where  $\mu_{BP} \sim (T / 300\text{K})^{-2.4}$  [16], [17]. More detailed discussions of the new model and its numeric implementation can be found in [14].

The reduction of the channel mobility due to Coulomb scattering at the interface charges was considered in the form as implemented in Sentaurus Device [18]

$$\mu_C = \frac{\mu_i \left( \frac{T}{300 \text{ K}} \right) \left\{ 1 + \left[ c / (c_{trans} \left( \frac{N_c}{N_0} \right)^{\eta 1} ) \right]^v \right\}}{\left( \frac{N_c}{N_0} \right)^{\eta 2} D(x) f(E_\perp)} \quad (10)$$

where  $\mu_i$  is a fitting parameter,  $c$  the concentration of the electrons near the interface,  $N_c$  the density of interface traps,  $x$  the distance from the interface, and  $E_\perp$  the electric field perpendicular to the oxide/semiconductor interface. The functions  $D(x)$  and  $f(E_\perp)$  are given by

$$D(x) = e^{-x/l_{crit}} \quad (11)$$

$$f(E_\perp) = 1 - e^{[-(E_\perp/E_0)^{\gamma}]}, \quad (12)$$

The parameters  $\mu_i$ ,  $N_0$ ,  $\eta 1$ ,  $\eta 2$ ,  $\nu$ ,  $l_{crit}$ ,  $E_0$ , and  $\gamma$  were used with the default values of the model parameters taken from Si in Sentaurus Device. To reproduce the experimentally measured dependence of the mobility on the doping concentration, the model had to be calibrated for each  $N_A$ . For this purpose, the parameter  $c_{trans}$  representing the screening of the carriers in the inversion layer was adjusted. By fitting the simulations to the measurements, following values of  $c_{trans}$  have been obtained:  $2.8 \cdot 10^{16}$  cm<sup>-3</sup>,  $8 \cdot 10^{16}$  cm<sup>-3</sup>,  $2.5 \cdot 10^{17}$  cm<sup>-3</sup> and  $1.55 \cdot 10^{18}$  cm<sup>-3</sup> for  $N_A$  equal to  $1 \cdot 10^{15}$  cm<sup>-3</sup>,  $1 \cdot 10^{16}$  cm<sup>-3</sup>,  $5 \cdot 10^{16}$  cm<sup>-3</sup> and  $5 \cdot 10^{17}$  cm<sup>-3</sup>, respectively.

The contribution attributed to surface-roughness scattering was modeled in the form [18]

$$\mu_{SR} = \left\{ \frac{(E_\perp/E_{ref})^2}{\delta} + \frac{E_\perp^3}{\eta} \right\}^{-1} \frac{1}{D} \quad (13)$$

where  $E_{ref}$  is the reference electric field equal to 1 V/cm, while  $\delta$  and  $\eta$  are fitting parameters which depend on the roughness of the SiC/SiO<sub>2</sub> interface. The lower the roughness of the interface, the higher the values of  $\delta$  and  $\eta$ .

Considering the dependence of  $\mu_{SR}$  on the electric field  $E_\perp$ , the contribution of surface-roughness scattering is stronger at higher gate voltages. Taking this into account, the values of  $\delta$  and  $\eta$  were modified from the Si default values by bringing the simulated and measured drain currents at higher  $V_G$  into agreement. The values of  $\delta$  and  $\eta$  were found to be equal to  $1.7 \cdot 10^{13}$  cm<sup>2</sup>/Vs and  $1.7 \cdot 10^{29}$  V<sup>2</sup>/cm s for the MOSFET with  $N_A = 5 \cdot 10^{17}$  cm<sup>-3</sup> and  $t_{ox} = 34$  nm. For the three other MOSFETs with  $t_{ox} = 25.5$  nm,  $\delta$  and  $\eta$  are equal to  $1.6 \cdot 10^{14}$  cm<sup>2</sup>/Vs and  $1.6 \cdot 10^{30}$  V<sup>2</sup>/cm s, respectively. It can be seen that the fitting parameters for the MOSFETs with different oxide thicknesses differ almost by a factor of 10, indicating that the MOSFET with the thicker oxide has a rougher interface than the MOSFET with the thinner oxide. This result is in agreement with the work of Y. Chen and et al. [19], where it was shown that with increasing oxide thickness the roughness of the interface increases.

Finally, the contribution attributed to the surface-phonon scattering was modeled in the form [18]

$$\mu_{SP} = \left\{ \frac{B}{E_\perp} + \frac{CN_A^{\alpha 1}}{E_\perp^{1/3} T} \right\} \frac{1}{D} \quad (14)$$

The model parameters  $B$ ,  $C$ , and  $\alpha 1$  in our simulations of 4H-SiC MOSFETs were taken from the literature [20].

### B. Reproduction of the current-voltage characteristics

Applying interface-trap and mobility-degradation models as described in the previous section, the current-voltage characteristics have been simulated numerically first at 300 K. A comparison of the simulations and measurements is shown in Fig. 4 for the four studied MOSFETs. As it can be seen, the models used in the simulations excellently reproduce the doping dependence of the measured drain current at room temperature. Changing the temperature has two direct effects: Firstly, all contributions of the scattering mechanisms to the

channel mobility change according to their temperature dependence. Secondly, the bulk potential changes and with it the occupation of the interface traps. Both are taken into account accordingly in Sentaurus Device when the nominal device temperature is changed. A comparison of the simulations and measurements is shown in Figs. 5 and 6 for the MOSFETs with  $N_A$  equal to  $5 \cdot 10^{17} \text{ cm}^{-3}$  and  $1 \cdot 10^{15} \text{ cm}^{-3}$ , respectively.

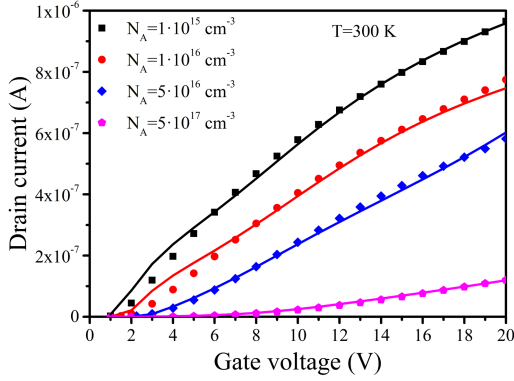


Fig. 4. Comparison of the simulated (lines) and measured (symbols) drain current for the MOSFETs with different  $N_A$ .

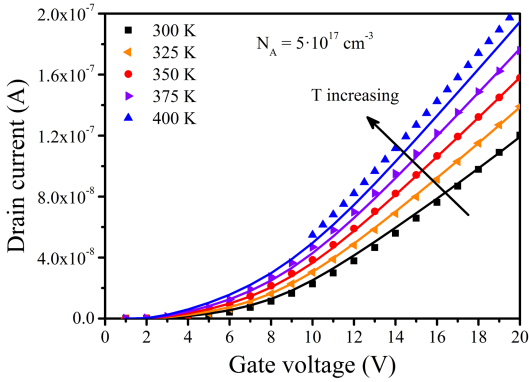


Fig. 5. Temperature dependence of the simulated (lines) and measured (symbols) drain current for the MOSFET with  $N_A = 5 \cdot 10^{17} \text{ cm}^{-3}$ .

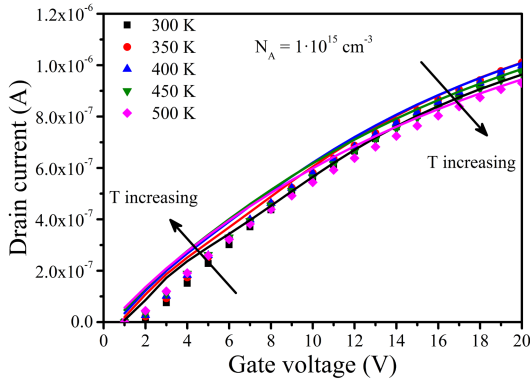


Fig. 6. Temperature dependence of the simulated (lines) and measured (symbols) drain current for the MOSFET with  $N_A = 1 \cdot 10^{15} \text{ cm}^{-3}$ .

As it can be seen, the models used in the simulation can also very well reproduce the temperature dependence of the current-voltage measurements for the MOSFETs with low and high  $N_A$ . From the comparison of the current-voltage characteristics in Fig. 5 and Fig. 6 it can be seen that the

temperature dependence of the drain currents depends strongly on the background doping concentration. At high  $N_A$ , the drain current strongly increases in the studied temperature range with increasing temperature, while at low  $N_A$  it is almost independent of temperature showing a slight increase at low gate voltages and a slight decrease at high gate voltages.

### C. Interpretation of Hall-effect measurements

Hall-effect measurement is one of the straight-forward methods to characterize experimentally transport properties in the channel of SiC MOSFETs. However, it is clear from (2) and (3) that the drift-channel mobility  $\mu$  and the sheet carrier density  $n_{inv}$  obtained are just as accurate as the Hall factor. Currently, it is common practice to assume  $r_H$  being equal to unity [12]. However, in our previous works, it has been shown that the Hall factor in the channel of SiC MOSFETs differs significantly from unity and, moreover, depends on the gate voltage applied [21]. Thus, based on our recently developed method [22], the Hall factor in the studied SiC MOSFETs has been calculated at different doping concentrations and temperatures. The results of the calculation are shown in Figs. 7 and 8 for the MOSFETs with  $N_A$  values of  $5 \cdot 10^{16} \text{ cm}^{-3}$  and  $1 \cdot 10^{16} \text{ cm}^{-3}$  for 300 K as well as with  $N_A$  values of  $1 \cdot 10^{15} \text{ cm}^{-3}$  and of  $5 \cdot 10^{17} \text{ cm}^{-3}$  in the temperature range from 300 K till 500 K and from 300 K till 400 K, respectively.

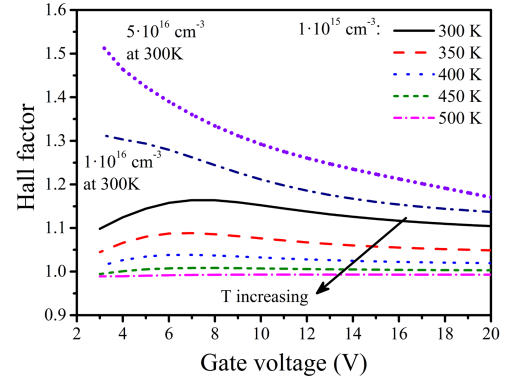


Fig. 7. Hall factor for the electron transport in the channel of SiC MOSFETs with  $N_A$  value of  $1 \cdot 10^{15} \text{ cm}^{-3}$  in the temperature range from 300 K till 500 K and with  $N_A$  values of  $1 \cdot 10^{16} \text{ cm}^{-3}$  and  $5 \cdot 10^{16} \text{ cm}^{-3}$  at 300 K.

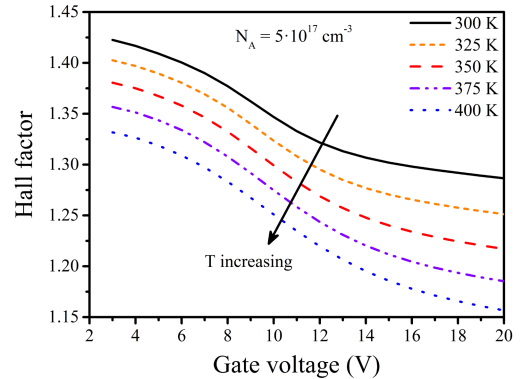


Fig. 8. Hall factor for the electron transport in the channel of SiC MOSFETs with  $N_A$  values of  $5 \cdot 10^{17} \text{ cm}^{-3}$  at different temperatures.

In addition to the dependence of the Hall factor on the gate voltage, discussed in our previous work [21], the Hall factor

depends on doping concentration and temperature. With decreasing  $N_A$ , the Hall factor also decreases, which can be mainly related to a decrease of Coulomb scattering at interface charges. A decrease of the Hall factor is seen also with increasing temperature. Taking the results in Figs. 7 and 8 and using (2) and (3), the results of the Hall-effect measurements have been corrected with the calculated Hall factor. A comparison between simulated and measured sheet carrier density for different doping concentrations and temperatures has been published elsewhere [14], [23]. Here, we focus only on channel mobility and scattering mechanisms. A comparison of the channel mobility from the simulation and Hall-factor-corrected measurements is shown in Fig. 9 for room temperature. The values of the simulated mobility were derived from the simulated current-voltage characteristics shown in Fig. 4 and the simulated sheet carrier density using

$$\mu = \frac{I_D L}{q W V_D n_{inv}} \quad (15)$$

where  $L$  and  $W$  are the channel length and width, respectively.

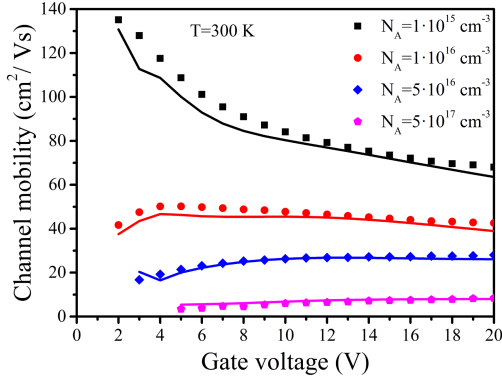


Fig. 9. Comparison of the channel mobility from the simulations (lines) and Hall-factor-corrected measurements (symbols) for the MOSFETs with different  $N_A$  at 300 K.

The very good agreement in Fig. 9 between the simulated and measured results for 300 K allows to apply this simulation methodology further to the temperature dependence of the transport properties in the channel of SiC MOSFETs. A comparison of the simulated and Hall-factor-corrected channel mobility for the MOSFETs with  $N_A$  values of  $5 \cdot 10^{17} \text{ cm}^{-3}$  and  $1 \cdot 10^{15} \text{ cm}^{-3}$  at different temperatures is shown in Fig. 10.

For the lower  $N_A$ , it can be seen in Fig. 10b that the simulated channel mobilities reproduce the Hall-factor-corrected measurements very well for all temperatures. For the higher  $N_A$  in Fig. 10a, the agreement is less perfect but the trends are well reproduced. This indicates that there is further potential for the improvement of the mobility models used. Overall, the good agreement between the simulations and measurements shown in Sections B and C confirms the self-consistency of the simulation methodology developed in the current work. Thus, the simulation results can be used further to study the effects of doping concentrations and temperatures upon the scattering mechanisms.

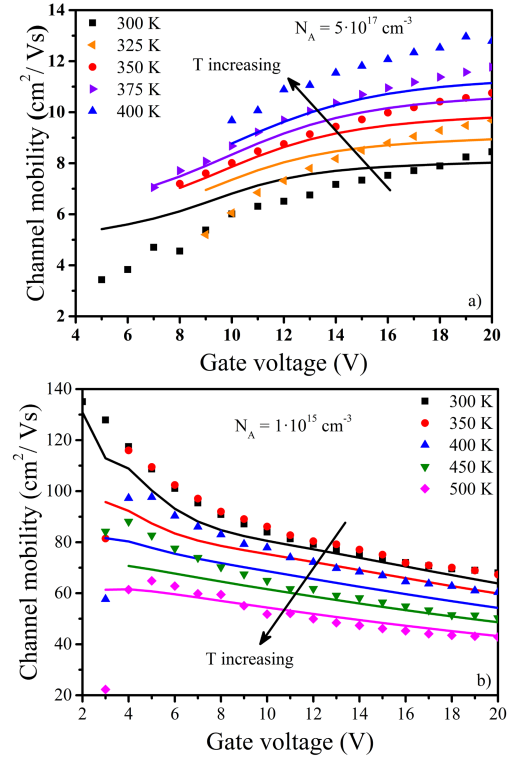


Fig. 10. Comparison of the channel mobility from the simulations (lines) and Hall-factor-corrected measurements (symbols) for the MOSFETs with  $N_A$  values of  $5 \cdot 10^{17} \text{ cm}^{-3}$  (a) and  $1 \cdot 10^{15} \text{ cm}^{-3}$  (b) at different temperatures.

## V. DISCUSSIONS

To analyze the scattering mechanisms in the channel of SiC MOSFETs and, thus, to understand the difference in the temperature dependences of the channel mobility, the mobility components have been calculated for different  $N_A$  and at different temperatures. This calculation has been performed using the method of small variations [14] based on the numerical simulation of the current-voltage characteristics which excellently reproduce the measured ones, as it was shown in Figs. 4 – 6. It should be noted that a splitting of the channel mobility into components allows to assess the relative contributions of the scattering mechanisms to the total mobility. The results of the extraction of the mobility components in the channel of SiC MOSFETs with  $N_A$  values of  $5 \cdot 10^{17} \text{ cm}^{-3}$  and of  $1 \cdot 10^{15} \text{ cm}^{-3}$  at room temperature are shown in Figs. 11 and 12, respectively. For an easier comparison of the impact of all scattering mechanisms upon the total mobility, the inverse mobility is depicted.

In Fig. 11 it can be seen that the inverse mobility components associated with Coulomb scattering at ionized impurities in the bulk as well as with bulk-phonon and surface-phonon scattering are much lower than the inverse total mobility. This indicates their negligibility for the total channel mobility and, as a consequence, for the performance of SiC MOSFETs with high  $N_A$ . In contrast, the inverse mobility associated with Coulomb scattering at the interface charges and surface-roughness scattering are the predominant scattering mechanisms.

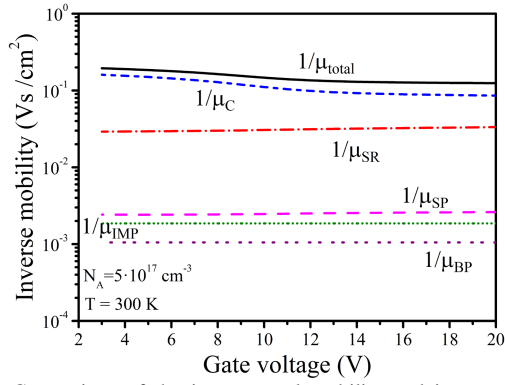


Fig. 11. Comparison of the inverse total mobility and inverse mobility components for MOSFET with  $N_A$  values of  $5 \cdot 10^{17} \text{ cm}^{-3}$  at  $T = 300 \text{ K}$ .

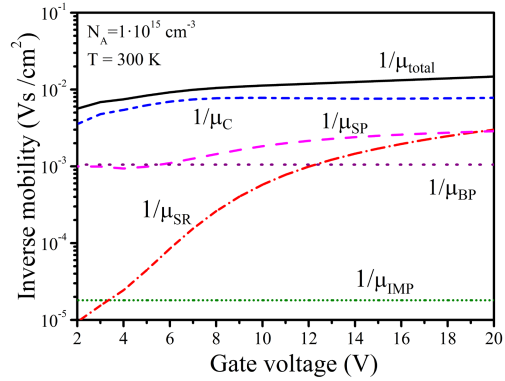


Fig. 12. Comparison of the inverse total mobility and inverse mobility components for MOSFET with  $N_A$  values of  $1 \cdot 10^{15} \text{ cm}^{-3}$  at  $T = 300 \text{ K}$ .

For the SiC MOSFET with the lowest  $N_A$ , shown in Fig. 12, there are two main differences in the contributions of the scattering mechanisms to the channel mobility. The first one is that Coulomb scattering at the interface charges is on average by a factor of 10 lower than in the MOSFET with the highest  $N_A$ . The decrease of Coulomb scattering at the interface charges with decreasing doping concentration is reflected in an increase of the channel mobility, shown also in Fig. 9 for different  $N_A$ . A common explanation for this effect is that a decrease of  $N_A$  leads to a decrease of the bulk potential and, as a consequence, of the occupation of the interface traps. Thus, the higher channel mobility at lower  $N_A$  is often explained only by the lower amount of the charged interface traps. However, we found that an increase of the channel mobility with decreasing  $N_A$  requires a broader view. One of the effects which have to be considered is the widening of the channel with decreasing  $N_A$ . Moving from the interface to the SiC bulk, charged interface traps have less impact on the mobility due to the quick decrease of the Coulomb potential which is screened by the inversion electrons. Thus, the mobility is expected to increase strongly when the channel gets wider. The second difference is that in the MOSFET with the lowest  $N_A$  surface-phonon scattering contributes to the channel mobility much stronger than in the MOSFET with the highest  $N_A$  and can be considered the second-most important scattering mechanism. This can be one of the explanations for the results shown in Fig. 1, where surface-phonon scattering

describes well the trend of the Hall mobility with respect to the effective field.

In addition to the analysis performed at 300 K, the most relevant mobility components for the temperature dependence, i.e.  $\mu_C$ ,  $\mu_{SP}$  and  $\mu_{BP}$ , have been calculated at 400 K and compared in Fig. 13 with the calculations for 300 K.

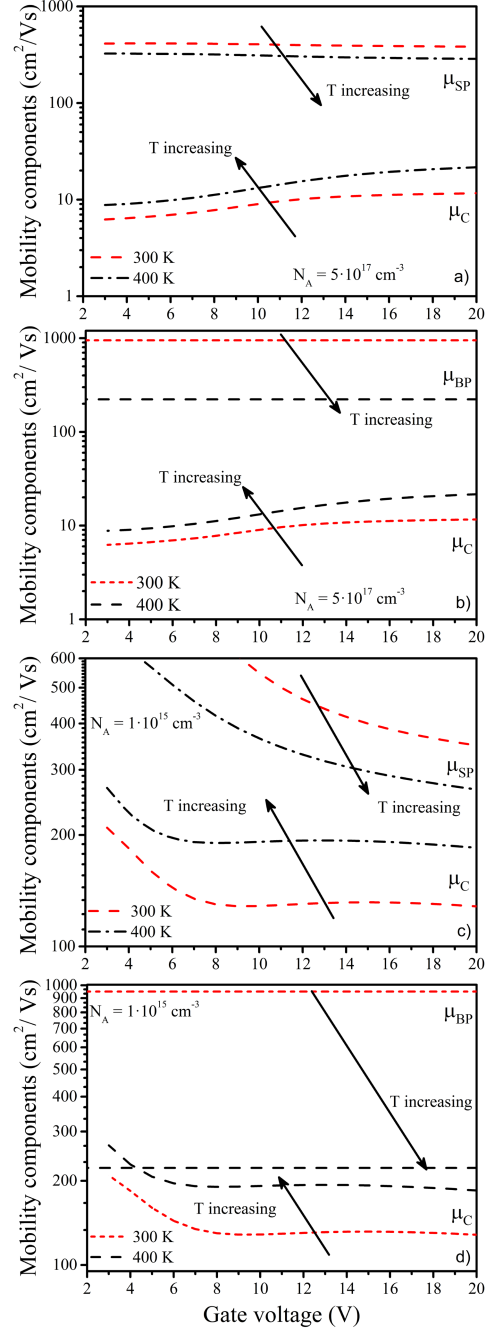


Fig. 13. Temperature and gate voltage dependence of the mobility components  $\mu_C$ ,  $\mu_{SP}$  and  $\mu_{BP}$  for the MOSFETs with  $N_A$  values of  $1 \cdot 10^{15} \text{ cm}^{-3}$  and of  $5 \cdot 10^{17} \text{ cm}^{-3}$ .

In Fig. 13 it can be seen that  $\mu_C$  increases strongly with increasing temperature which confirms the expected decrease of Coulomb scattering at interface charges. This can be explained mainly by two interrelated effects. The first one is a decrease in the amount of charged traps due to the decrease of

the bulk potential with temperature. The second one is an increase of the screening of the scattering centers due to the increase of the concentration of the inversion electrons. In contrast to Coulomb scattering, surface-phonon and bulk-phonon scattering increase with increasing temperature. As a consequence, the respective mobility components decrease.

A comparison of the mobility components at different temperatures with their total mobilities explains the change of the temperature dependence of the channel mobility for the MOSFETs with high and low  $N_A$  as follows: The mobility component  $\mu_{SP}$  at high gate voltages has the same order of magnitude, as it can be seen in Fig. 13, for both lightly and highly doped channels. Bulk-phonon scattering increases for both with increasing temperature. However, Coulomb scattering at the interface charges is at 300 K much stronger in the highly doped MOSFET than in the lowly doped one, as it was discussed above. In fact, in the MOSFETs with the high  $N_A$ , Coulomb scattering at the interface charges is so strong that the contributions of surface-phonon and bulk-phonon scattering are still negligible at 400 K. This means that for the temperature dependence of the SiC MOSFET with the high  $N_A$ , at least in the temperature range from 300 till 400 K, only Coulomb scattering plays a fundamental role. This leads to an increase of the channel mobility and, as a consequence, of the drain current with increasing temperature. In case of the MOSFET with the low  $N_A$ , where Coulomb scattering is relatively low in comparison with the MOSFET with high  $N_A$ , an increase in temperature leads to the effect that the contributions of surface-phonon and bulk-phonon scattering become significant. Considering that the temperature dependence of bulk-phonon scattering is stronger than the temperature dependence of surface-phonon scattering,  $\mu_{BP}$  decreases with increasing temperature faster and starts to dominate at high temperatures. This results in the reduction of the channel mobility as well as the drain current at high temperatures in lightly doped channels of SiC MOSFETs.

## VI. CONCLUSIONS

To investigate electron scattering mechanisms in lateral n-channel 4H-SiC MOSFETs with different channel doping concentrations, current-voltage and Hall-effect measurements have been performed as a function of temperature. To interpret the electrical measurements, a self-consistent TCAD simulation methodology has been developed which includes the calculation of the Hall factor in the channel, an improved method for the extraction of the interface trap density as a function of trap energy from measurements, and a new bulk-mobility model. Based on the good agreement between the simulations and measurements, explanations for the effects of doping and temperature upon the scattering mechanisms and further on the temperature dependence of the drain current have been obtained.

## REFERENCES

[1] P. Deak, J. M. Knaup, T. Hornos, Ch. Thill, A. Gali, and T. Frauenheim, "The mechanism of defect creation and passivation at the SiC/SiO<sub>2</sub> interface", *J. Appl. Phys.*, vol.40, no.20, pp. 6242-6253, 2007.

[2] G. Ortiz, C. Strenger, V. Uhnevionak, A. Burenkov, A. J. Bauer, P. Pichler, F. Cristiano, E. Bedel-Pereira, and V. Mortet, "Impact of Acceptor Concentration on Electrical Properties and Density of Interface States of 4H-SiC n-Metal-Oxide-Semiconductor Field Effect Transistors Studied by Hall Effect", *Appl. Phys. Lett.*, vol. 106, no. 6, 2015, Art. ID 062104.

[3] P. Jamet, S. Dimitrijevic, and P. Tanner, "Effects of nitridation in gate oxides grown on 4H-SiC," *J. Appl. Phys.*, vol. 90, no. 10, p. 5058-5063, 2001.

[4] L. A. Lipkin, M. K. Das, and J. W. Palmour, "N<sub>2</sub>O processing improves the 4H-SiC:SiO<sub>2</sub> interface," *Mater. Sci. Forum*, vol. 389-393, pp. 985-988, 2002.

[5] K. Matocha, "Challenges in SiC power MOSFET design," *Solid-State Electronics*, vol. 52, no. 10, pp. 1631-1635, 2008.

[6] S.-H. Ryu, S. Dhar, S. K. Haney, A. Agarwal, A. J. Lelis, B. Geil, and C. J. Scozzie, "Critical issues for MOS based power devices in 4H-SiC," *Mater. Sci. Forum*, vol. 615-617, pp. 743-748, 2009.

[7] C. Strenger, "Herstellung und Charakterisierung von Metall-Oxid-Halbleiter-kondensatoren und Feldeffekttransistoren auf 4H-Siliciumcarbid", Ph.D dissertation, Univ. Erlangen-Nuremberg, 2015.

[8] C. Strenger, V. Häublein, T. Erlbacher, A. J. Bauer, H. Ryssel, A. M. Beltran, S. Schamm-Chardon, V. Mortet, E. Bedel-Pereira, M. Lefebvre and F. Cristiano, "Comparative study of electrical and microstructural properties of 4H-SiC MOSFETs," *Mater. Sci. Forum*, vol. 717-720, pp. 437-440, 2012.

[9] S. Dhar, S. Haney, L. Cheng, S.-R. Ryu, A. K. Agarwal, L. C. Yu, and K. P. Cheung, "Inversion layer carrier concentration and mobility in 4H-SiC metal-oxide-semiconductor field-effect transistors," *J. Appl. Phys.*, vol. 108, no. 5, 2010, Art. ID 054509.

[10] S. Potbhare, N. Goldsman, G. Pennington, A. Lelis, and J. M. McGarrity, "Numerical and experimental characterization of 4H-silicon carbide lateral metal-oxide-semiconductor field-effect transistor," *J. Appl. Phys.*, vol. 100, no. 4, 2006, Art. ID 044515.

[11] V. Tilak, "Inversion layer electron transport in 4H-SiC metal-oxide-semiconductor field-effect transistors," in *Silicon carbide: Power devices and sensors*, pp. 267-290, Wiley-VCH, Germany, 2010.

[12] C.-Y. Lu, J. A. Cooper, T. Tsuji, G. Chung, J.R. Williams, K. McDonald, and L.C. Feldman, "Effect of process variations and ambient temperature on electron mobility at the SiO<sub>2</sub>/4H-SiC interface", *IEEE Trans. Electron Devices*, vol. 50, no.7, pp. 1582-1588, 2003.

[13] V. Tilak, K. Matocha, and G. Dunne, "Electron-scattering mechanisms in heavily doped silicon carbide MOSFET inversion layers," *IEEE Trans. Electron Devices*, vol. 54, no. 11, pp. 2823-2829, 2007.

[14] V. Uhnevionak, "Simulation and Modeling of Silicon Carbide Devices," Ph.D. dissertation, Univ. Erlangen-Nuremberg, 2015, <http://nbn-resolving.de/urn:nbn:de:bvb:29-opus4-61975>.

[15] V. Uhnevionak, C. Strenger, A. Burenkov, V. Mortet, E. Bedel-Pereira, J. Lorenz, P. Pichler, "Characterization of n-channel MOSFETs: Electrical measurements and simulation analysis", *ESSDERC 2013*, IEEE, pp. 242-245, 2013.

[16] M. Roschke and F. Schwierz, "Electron mobility models for 4H, 6H, and 3C SiC MESFETs," *IEEE Trans. Electron Devices*, vol. 48, no. 7, pp. 1442-1447, 2001.

[17] D. Stefanakis and K. Zekentes, "TCAD models of the temperature and doping dependence of the bandgap and low field carrier mobility in 4H-SiC," *Microelectronic Engineering*, vol. 116, pp. 65-71, 2014.

[18] Synopsys, Inc., *Sentaurus device user guide*. Mountain View, CA, 2010.

[19] Y. Chen, R. Myricks, M. Decker, J. Liu, and G.S Higashi, "The origination and optimization of Si/SiO<sub>2</sub> interface roughness and its effect on CMOS performance," *IEEE Electron Device Letters*, vol. 24, no. 5, pp. 295-297, 2003.

[20] A. Perez-Tomas, P. Brosselard, P. Godignon, and J. Millan, "Field-effect mobility temperature modeling of 4H-SiC metal-oxide-semiconductor transistors," *J. Appl. Phys.*, vol. 100, no. 11, 2006, Art. ID 114508.

[21] V. Uhnevionak, C. Strenger, A. Burenkov, V. Mortet, E. Bedel-Pereira, F. Cristiano, A. J. Bauer, P. Pichler, "Hall factor calculation for the characterization of transport properties in n-channel 4H-SiC MOSFETs," *Mater. Sci. Forum*, vol. 778-780, pp. 483-486, 2014.

[22] V. Uhnevionak, A. Burenkov, P. Pichler, "On the calculation of Hall factors for the characterization of electronic devices", 9th Conference on Ph.D. Research in Microelectronics and Electronics PRIME 2013, IEEE, pp. 241-244, 2013.

[23] V. Uhnevionak, A. Burenkov, C. Strenger, A. Bauer, and P. Pichler, "On the temperature dependence of the Hall factor in n-channel 4H-SiC MOSFETs," *ECS Transactions*, vol. 58, no. 4, pp. 81-86, 2013.



**Viktoriya Uhnevionak** received the Dipl. Eng.-Phys. degree in physics (engineering) from the Belarussian State University in Minsk, Belarus, in 2011 and the Ph.D. degree from Friedrich-Alexander University Erlangen-Nuremberg, Germany, in 2015. The main focus of her doctoral work was on modeling and simulation of silicon carbide (SiC) MOSFETs.



thermal processes.

**Fuccio Cristiano** received 1991 the B.Sc. degree in physics from the University of Catania, Italy, and 1998 the Ph.D. degree from the University of Surrey, U.K. Having worked as postdoc at CEMES/CNRS in Toulouse, France, he joined LAAS/CNRS in Toulouse in 2000. His recent work addresses in particular the defects' role on the electrical activation of dopants in silicon, especially after ultra-rapid



in microelectronics.

**Alexander Burenkov** received his Dipl. Phys. degree from the TU Dresden, Germany, in 1974, Cand. Sc. degree from the University of Rostov, Russia, in 1981, and Dr. Sc. from the Belarussian State University in Minsk, Belarus, in 1991. Since 1994 he is with the Fraunhofer IISB. His present research interest is 3D simulation of microelectronic devices and software development for technology modeling



(SiC).

**Anton J. Bauer** received his Diploma in physics from the University Regensburg, Germany, in 1988 and his Ph.D. in Electrical Engineering from the University Erlangen Nuremberg, Germany, in 1995. Since 1998, he heads the Technology and Manufacturing department at Fraunhofer IISB. His current research topics include power MOSFET development in Si as well as in silicon carbide



**Christian Strenger** received his Dipl.-Ing. degree in electrical engineering from the Technical University of Munich, Germany, in 2009 and his Dr.-Ing. from the University Erlangen Nuremberg, Germany, in 2014. Since 2013 he is with the Fraunhofer Institute of Integrated Systems and Device Technology in Erlangen, Germany. His present research interest is the development of power electronic devices on 4H-SiC.



**Peter Pichler** (SM'02) received 1982 the Dipl.-Ing. degree and 1985 the Dr. techn. degree from the TU Vienna, Austria. In 2004, he received the Venia Legendi from the University of Erlangen-Nuremberg, Germany. Since 1986, he has been Group Manager for doping and device simulation at Fraunhofer IISB. His present research interests include diffusion and activation phenomena in elemental and compound semiconductors.



works on magnetic nanoparticles for biological applications.

**Guillermo Ortiz** (M'15) received the B.S. in Physics and M.S. in Materials Physics' for Microelectronics from Université Montpellier II, France, in 2007 and 2009, respectively. In 2013 he received the Ph.D. from Université Toulouse III, France. After working as postdoc at CNRS/LAAS in Toulouse, France, he joined CEA/SPINTEC in Grenoble, France, where he



characterization for device optimization.

**Elena Bedel-Pereira** received her PhD degree from the University of Toulouse in 1984. Then, she worked at LAAS/CNRS laboratory, Toulouse France, as permanent scientist (CR-CNRS) since 1986. Having worked on the growth and characterization of III/V semiconductor materials and in the field of materials for nano-electronics, her research interest can be summarized as advanced



Republic.

**Vincent Mortet** received 2001 his Ph.D. degree in Physics from the University of Valenciennes and Hainaut-Cambrésis, France. He has been working at the Institute for Materials Research, Hasselt, Belgium and LAAS/CNRS, Toulouse, France. Since 2013 he is leading the Nanosystems and Biointerfaces (MNB) group in the Dpt. of Functional Materials of the Institute of Physics of the Academy of Sciences of the Czech